ELSEVIER

Further solid-phase microextraction–gas chromatography–mass spectrometry applications: "on-fibre" and aqueous photodegradation of nitro musks[☆]

L. Sanchez-Prado, M. Lores[*], M. Llompart, C. Garcia-Jares,
M. Lourido, R. Cela

Departamento de Química Analítica, Nutrición y Bromatología, Facultad de Química, Instituto de Investigación y Análisis Alimentario (IIAA), Universidad de Santiago de Compostela. Avda. das Ciencias S/N, Campus Sur, E-15782 Santiago de Compostela, Spain

Abstract

Photodegradation kinetics of four nitro musks (musk xylene, musk tibetene, musk ketone and musk moskene) in solid-phase microextraction (SPME) fibres ("photo-SPME") and in an aqueous system were studied by means of gas chromatography–mass spectrometry (MS) detection. Musks fragrances were extracted from aqueous solutions using SPME fibres that subsequently were exposed to different UV irradiation times, generating photoproducts easily characterized by their mass spectra. Aqueous photodegradation studies followed by SPME were also performed and compared to photo-SPME. The same fourteen photoproducts have been detected in both media. The potential of this approach to readily calculate apparent rate constants (from 10^{-4} to $10^{-3}\,\mathrm{s}^{-1}$), half-life times (from 3 to 32 min) and reaction orders ($n = 1$) in both media is stated. The main photoreaction determined was photocyclization, but products of photoreduction and photorearrangement have also been detected. Tentative photodegradation pathways for musk moskene and musk tibetene are proposed for the first time.
© 2004 Elsevier B.V. All rights reserved.

Keywords: Nitro musks; Photodegradation; Solid-phase microextraction; UV irradiation

1. Introduction

Nitro musks are synthetic compounds used on a grand scale as fragrance fixatives and materials in personal-care (PPCPs) and household products such as cosmetics, soaps, laundry detergents, fabric softeners, household cleaning products, air fresheners and so on, due to their fragrance properties [1]. Increasing environmental concern about the presence, especially in surface water samples, of artificial musk fragrances has attracted the attention of several authors [2–12]; since these substances are considered ubiquitous, persistent, bioaccumulative and sometimes highly toxic. Based on these properties, it is important to know the environmental degradation pathways of nitrated musk compounds. These substances are poorly degraded by the microorganisms, suggesting that abiotic transformations, e.g. photochemical degradation—constitute an alternative to decompose these compounds. Although, there is information concerning the photodegradation behaviour of nitrated musk compounds [13–17], all of these studies were performed in water or in organic solvents.

Solid-phase microextraction (SPME) has been recently proposed as an extraction technique for the analysis of musks compounds in water and sewage sludge samples, [3,7,12] due to its inherent advantages. At the same time, the possibility

of performing photochemical studies of environmentally concerning compounds (e.g. PCBs, DDT and other pesticides and polycyclic musks) in SPME fibres (photo-SPME) has been already demonstrated [18–22]. In photo-SPME, the target analytes are first extracted and then the photolysis takes place directly on the fibre, so the whole system (primary compounds and photoproducts) can be analysed simultaneously. All photoproducts are therefore generated "in situ" and remain in the fibre, avoiding further extraction steps and making easier their tentative identification by mass spectrometry (MS), due to the high concentration factors.

This work is an important contribution to the knowledge of nitro musks photochemical behaviour, characterizing their kinetics and identifying their photoproducts by solid-phase microextraction–gas chromatography–mass spectrometry detection, via an "on-fibre" photodegradation approach. In addition, in a more classical approach, photodegradation kinetics and photoproducts generated in water were also studied, but using SPME as an alternative extraction technique. The obtained data have been compared with the "on-fibre" results. The apparent first-order rate constants, half-life times and the photoreactions detected for the four studied compounds are also presented.

2. Experimental

2.1. Reagents

The musks compounds, 1-*tert*-butyl-3,5-dimethyl-2,4,6-trinitrobenzene (Musk Xylene [81-15-2]), 1-*tert*-butyl-3,5-dimethyl-2,6-dinitro-4-acetylbenzene (Musk Ketone [81-14-1]), 1-*tert*-butyl-3,4,5-trimethyl-2,6-dinitrobenzene (Musk Tibetene [145-39-1]) and 1,1,3,3,5-pentamethyl-4,6-dinitroindane (Musk Moskene [116-66-5]) were supplied by Promochem Iberia (Barcelona, Spain). Table 1 depicts all these chemical structures. Isooctane and acetone were purchased from Merck (Mollet del Vallés, Barcelona, Spain). All the solvents and reagents were analytical grade.

The SPME manual holder and fibres were obtained from Supelco (Bellefonte, PA, USA). In this work, 100 μm polydimethylsiloxane (PDMS) coated fibres were used. The fibres were conditioned following manufacturer recommendations.

The solvent of stock solutions was cyclohexane. Water solutions were prepared by addition of an acetone standard solution of the four model compounds. The correspondent concentrations of each analyte in working solutions were 20 ng/mL in experiments depicted as C1 and 1 ng/mL in C2 studies.

Table 1
Chemical structures, retention times and selected ions for the analysis of the target musk compounds. The obtained percentages of undegraded compound vs. UV irradiation are also shown for both photo-SPME and aqueous photodegradation experiments

Compound	Chemical structure	Irradiation time (min)	photo-SPME (%)	Water (%)
Xylene		0	100	100
		5	61.9	44.5
		10	49.6	9.5
		20[a]	–	1.7
		30	13.4	0.6
		60	5.5	0
Retention time (min)	14.50	Identification ions (*m/z*)		282[b], 265, 283
Moskene		0	100	100
		5	68.5	54.9
		10	59.5	20.9
		20[a]	–	3.7
		30	22.5	1.0
		60	8.6	0.8
Retention time (min)	14.67	Identification ions (*m/z*)		263[b], 264, 261
Tibetene		0	100	100
		5	67.2	65.9
		10	59.7	50.8
		20[a]	–	17.5
		30	31.2	8.0
		60	16.8	1.6
Retention time (min)	15.02	Identification ions (*m/z*)		251[b], 252, 115
Ketone		0	100	100
		5	67.4	49.8
		10	57.4	15.0
		20[a]	–	2.8
		30	25.8	0.7
		60	13.5	0.2
Retention time (min)	15.27	Identification ions (*m/z*)		279[b], 191, 280

[a] This irradiation time has not been evaluated in photo-SPME experiments.

[b] Quantification ion.

2.2. Solid-phase microextraction and photodegradation procedures

Microextraction experimental conditions have been adapted from a previous study [12]. A 5 mL-aliquot of a water sample containing the target compounds was placed in 22 mL headspace vials. The vial was sealed with a headspace aluminum cap with a PTFE-faced septum. Then the vial was immersed in a water bath at 100 °C and let to equilibrate for 5 min before extraction. After this time, the fibre was exposed to the headspace over the water (HS-SPME) for 30 min and thermally desorbed in the GC injection port for 5 min.

A lab photoreactor model was used for photolysis experiments [18–22]: two low-pressure mercury lamps (8–10 W) were combined in such an arrangement that allows an easy positioning of the subject to be irradiated. For "on-fibre" photodegradation experiments, after HS-SPME extraction, the SPME fibre with the analytes already absorbed was subjected to the 254 nm irradiation wavelength during the designed time (2–60 min) into an efficient hood to warrant adequate security conditions; subsequently, GC–MS analyses were carried out. For aqueous photodegradation experiments, 5 mL of an aqueous solution containing the nitro musks mixture were placed in synthetic quartz precision cells and submitted to UV radiation in the same way described above. After the designed irradiation time (2–60 min) the photolized solution were placed in 22 mL headspace vials and HS-SPME–GC–MS analyses were performed. For every set of experiments a control extraction (same SPME procedure but without irradiation) was carried out.

SPME is an equilibrium technique; this means that the analytes are not exhaustively extracted from the sample matrix, therefore the recovery is relate with the global equilibrium between the three phases present in the system (the sample, the headspace and the fibre coating); of course, the total amount of analyte extracted does not change in equal experimental conditions. Besides, on the contrary of other extraction techniques, the total amount extracted is injected into the analytical instrument. Thus, to convert peak area data in mass or concentration data when required, the only need is to inject standard solutions of known concentrations and to demonstrate the linearity of the SPME extraction method.

2.3. Dark and thermal tests

Dark tests were carried out placing the fibre inside a glass vial and covering the whole device with aluminum foil; the irradiation was kept as in the remainder experiments. For thermal tests, a lab heater kept at 50 °C was used, temperature high enough taking into account that inside the photoreactor the temperature never reaches more than ambient ±1 °C, due to the efficient cooling devices. These tests are carried out to ensure that any changes in analytical response are due to the action of photons.

2.4. Chromatographic conditions

Analyses were performed on a Varian 3800 gas chromatograph (Varian Chromatography Systems, Walnut Creek, CA, USA) equipped with a 1079 split/splitless injector and an ion trap spectrometer Varian Saturn 2000 (Varian Chromatography Systems) with an MS detector. Nitro musks were separated on a 25 m length × 0.25 mm i.d., VA-5MS column coated with a 0.25 μm film. The GC oven temperature program was: 40 °C hold 2 min, rate 15 °C/min to a final temperature of 280 °C, hold for 5 min. Helium was employed as carrier gas, with a constant flow rate of 1.3 mL/min. Injector was programmed to return to the split mode after 2 min from the beginning of a run. Split flow was set at 50 mL/min. Injector temperature was held constant at 270 °C. Trap, manifold and transfer-line temperatures were 200 °C, 50 °C and 280 °C, respectively. The GC–MS system was operated by Saturn GC–MS workstation v5.4 software. The MS detection method was adapted from [12], increasing the mass range to 500 *m/z* to seek for heavier photoproducts. Table 1 shows retention times and identification and quantification ions for the selected musk fragrances.

3. Results and discussion

3.1. Preliminary experiments

Although other coatings showed better extraction efficiencies for the target compounds at the selected experimental conditions (HS-SPME at 100 °C) [12], PDMS SPME fibres were used in this study. Previous photo-SPME studies [18–22], where it has been stated that photodegradation only takes place, in an appreciable extent, using that commercial coating under the selected irradiation conditions (low pressure mercury lamps, 18 W), support this selection. Nevertheless, sensibility of PDMS–SPME fibres for nitro-musk compounds is acceptable and the detection limits are sufficiently low to permit photochemical studies of the selected compounds and to identify photoproducts.

Dark and thermal tests have been carried out to confirm that there are no losses of analytes through volatilisation and/or thermal degradation. Thus, four water solutions containing the nitro musks mixture were sequentially extracted and each one was subjected to different treatments: standard SPME (the fibre is immediately desorbed in the GC injector); dark test; thermal test and UV irradiation. All of them were carried out as it is described in Section 2. The obtained results in these tests demonstrated that the reduction of analytical response only took place in the UV irradiation experiments, confirming the photodegradation of the target analytes; remaining less than 40% of the parent compound after 30 min of UV irradiation. Results are shown in Fig. 1.
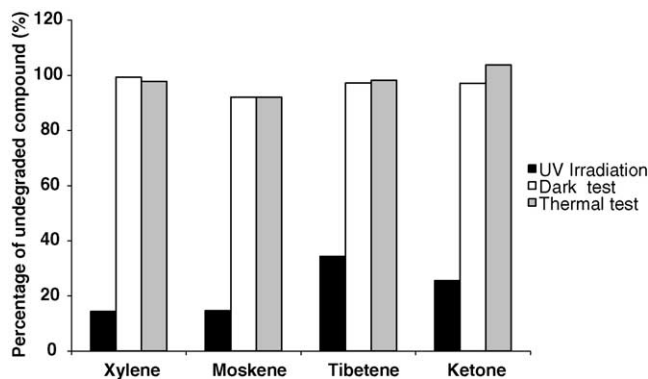
Fig. 1. Comparative results obtained for UV irradiation ($\lambda = 254$ nm), dark test and thermal test for the evaluated nitrated musk compounds.

3.2. Influence of irradiation time and kinetic studies

The preliminary experiments demonstrated that all nitrated musk compounds were photochemically degradable under the selected experimental conditions. Peak area changes for each individual compound after UV exposure have been evaluated, as it is shown in the chromatograms of Fig. 2 for two selected irradiation times. The four nitro musks showed comparable photodegradation behaviours. The obtained results in photo-SPME are expressed as percentage of undegraded compound (Table 1). The correspondent data from aqueous photodegradation experiments of nitro musks are also shown (Table 1). Photochemical reactions, both "on-fibre" and in aqueous media, follow first-order kinetics, indicating that the decrease in reagent concentration is an exponential function of irradiation time.

The rate constants and half lives for both systems were calculated (Table 2). The apparent first-order rate constants
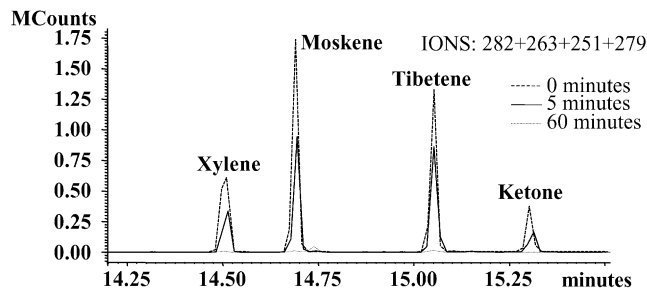

Fig. 2. Ion chromatograms showing the nitro musks "on-fiber" photodegradation.

(k_{ap}) of the photodegradation for each particular nitro musk has been determined as the slopes of the straight line equations obtained from linear regression: $\ln C$ versus time plot ($\ln C = -k_{ap}t + \ln C_0$), with squared regression coefficients mostly greater than 0.98 (Table 2). The correspondent half-life times (when the reagent species concentration is reduced to 50% of its initial amount) were also calculated using the expression: $t_{1/2} = \ln 2/k_{ap}$, only applicable for first-order reactions. Two series of experiments departing from different musks initial concentrations (C_1 and C_2) have been carried out and calculations were made for the two sets of data, determining the total reaction order (n) by the "half-life time comparison method":

$$n = 1 + \frac{\ln (t_{1/2})_1 - \ln (t_{1/2})_2}{\ln C_2 - \ln C_1}$$

giving values close to the unity in all cases (Table 2).

The apparent first-order rate constants (k_{ap}) were similar independently of the initial concentration, as it should be in first-order reactions. Rate constants in the order of 10^{-4} s^{-1} have been determined in photo-SPME experiments

Table 2
Experimental values of the apparent first-order rate constants, half-life times and reaction orders for the nitro musks studied

Compound	"On-fiber" experiments			Aqueous photodegradation		
	C_1	C_2	n[a]	C_1	C_2	n[a]
Xylene						
k_{ap} (s^{-1})	0.0007	0.0008		0.0030	0.0032	
$t_{1/2}$ (s)	985	923	0.98	230	218	0.98
R^2	0.9939	0.9718		0.9930	0.9943	
Moskene						
k_{ap} (s^{-1})	0.0006	0.0007		0.0017	0.0024	
$t_{1/2}$ (s)	1249	1051	0.93	418	284	0.87
R^2	0.9873	0.9859		0.9893	0.9844	
Tibetenee						
k_{ap} (s^{-1})	0.0004	0.0005		0.0014	0.0014	
$t_{1/2}$ (s)	1924	1496	0.93	497	485	0.99
R^2	0.9964	0.9675		0.9956	0.9728	
Ketone						
k_{ap} (s^{-1})	0.0006	0.0006		0.0026	0.0030	
$t_{1/2}$ (s)	1127	1257	1.03	271	231	0.94
R^2	0.9883	0.9793		0.9943	0.9908	

[a] n, total reaction order.

Table 3
Retention times and characteristic ions of the photoproducts obtained in both media

Photoproduct key	Retention time (min)	Quantification ion (*m/z*, %)	Identification ions (*m/z*, %)	Xylene	Moskene	Tibetene	Ketone
P1	10.03	218 (100)	218,172 (21), 157 (20)		+		
P2	10.88	236 (100)	236, 251(8), 162 (6)			+	
P3	11.30	215 (100)	215, 187 (51), 170 (30)			+	
P4	11.75	231 (100)	231, 203 (53), 188 (26)			+	
P5	11.80	233 (100)	233, 216 (18), 248 (7)			+	
P6	12.18	233 (100)	233, 187 (98), 245 (25)			+	
P7	12.21	234 (100)	234, 188 (42), 173 (38)		+		
P8	12.27	245 (100)	245, 260 (12), 203 (10)		+		
P9	12.73	219 (100)	219, 234 (30), 173 (15)		+		
P10	12.83	261 (100)	261, 115 (24), 276 (17)				+
P11	13.00	233 (100)	233, 248 (50), 187 (42)			+	
P12	13.39	233 (100)	233, 187 (35), 262 (10)		+		
P13	13.65	231 (100)	231, 248 (50), 203 (38)			+	
P14	13.85	262 (100)	262, 279 (90), 172 (26)	+			

Individual experiments were only carried out by photo-SPME.

and $10^{-3}\,\mathrm{s}^{-1}$ in aqueous photodegradation experiments for all the nitrated musk compounds, suggesting that transformation kinetic is about one order of magnitude faster in water that on SPME coating. However, the rank in the k_{ap} on each media is the same, as it is demonstrated by a Spearman coefficient equal to unity. Consequently with k_{ap} values, half-life times varied from about 900 to 1900 s "on-fibre" and between 200 and 400 s in aqueous media. Butte et al. [16] reported rate constants in water of the same order than our aqueous data: supposedly, the higher power of irradiation lamp (150 W) could compensate the lower energy from the longer irradiation wavelengths they used. When H_2O_2 is added as oxidizing agent to combine with 254 nm UV irradiation [17], the photochemical degradation rate constants in water are about two to three orders of magnitude higher.

3.3. Identification of photoproducts

Fourteen different photoproducts were generated during the irradiation of nitro musks mixture "on-fibre" and in aqueous photodegradation experiments. The chemical structure of eight molecules has been determined based on their mass spectra and two of them were surely identified based also on data already published [13,14]. Individual studies, though only for "on-fibre" experiments, confirmed the origin of the photogenerated compounds detected in each particular case (indicated with a "+" sign in Table 3); their retention times and their identification and quantification ions with the correspondent relative abundances are also included.

3.3.1. Xylene photoproducts

P14, the only photoproduct detected upon UV irradiation of xylene (Table 3), was identified as 3,3,5,7-tetramethyl-4,6-dinitro-2-indolinone and it is one of the photoproducts identified by Zhao and Schwack [13] both in cyclohexane irradiation and on a layer of cellulose stearate, used as clothes simulator, and by Butte et al. [16] in water. The chemical
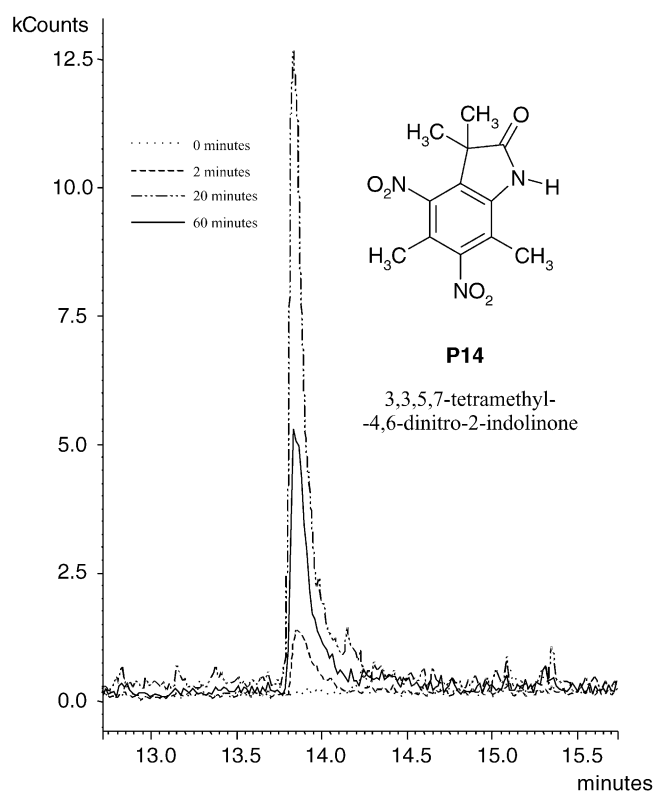

Fig. 3. Chemical structure and ion chromatograms at different irradiation times for the photoproduct detected in the photodegradation of musk xylene (P14).

structure of this compound and the correspondent ion chromatograms for three selected irradiation times are shown in Fig. 3. P14 is a photocyclization product originated from intramolecular attack of an electronically excited nitro group on the neighbouring *tert*-butyl group.

3.3.2. Moskene photoproducts

Up to date, there are no previous studies concerning musk moskene photodegradation pathways, and there is only a sug-
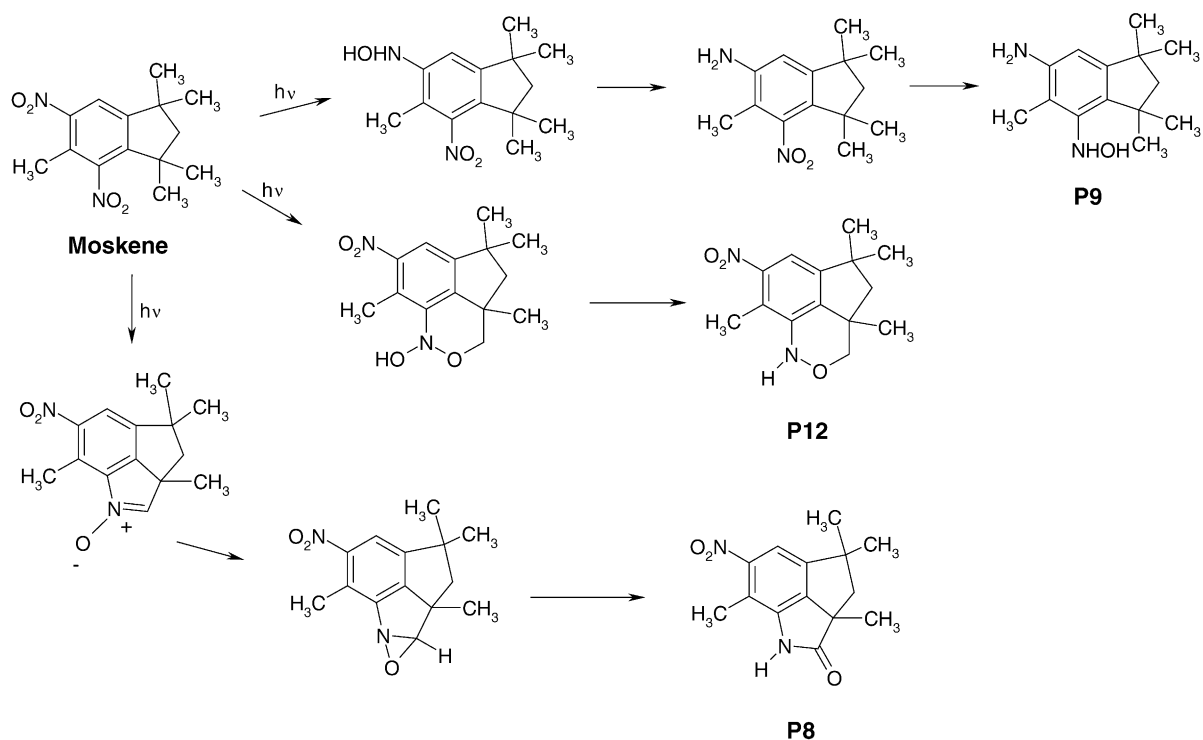
Fig. 4. Proposed photodegradation pathways for musk moskene.

gestion of an intermolecular dimerisation similar to that proposed by Butte et al. [16] for the musk ambrette. In this study, chemical structures of three photoproducts of moskene (P8, P9 and P12) and its photodegradation pathways are proposed

(Fig. 4) based on data about photodegradation of musks xylene and ketone [13,14], considering that chemical structures of all nitro musk compounds are similar, and by the obtained photoproducts mass spectra. There was no evidence of dimer
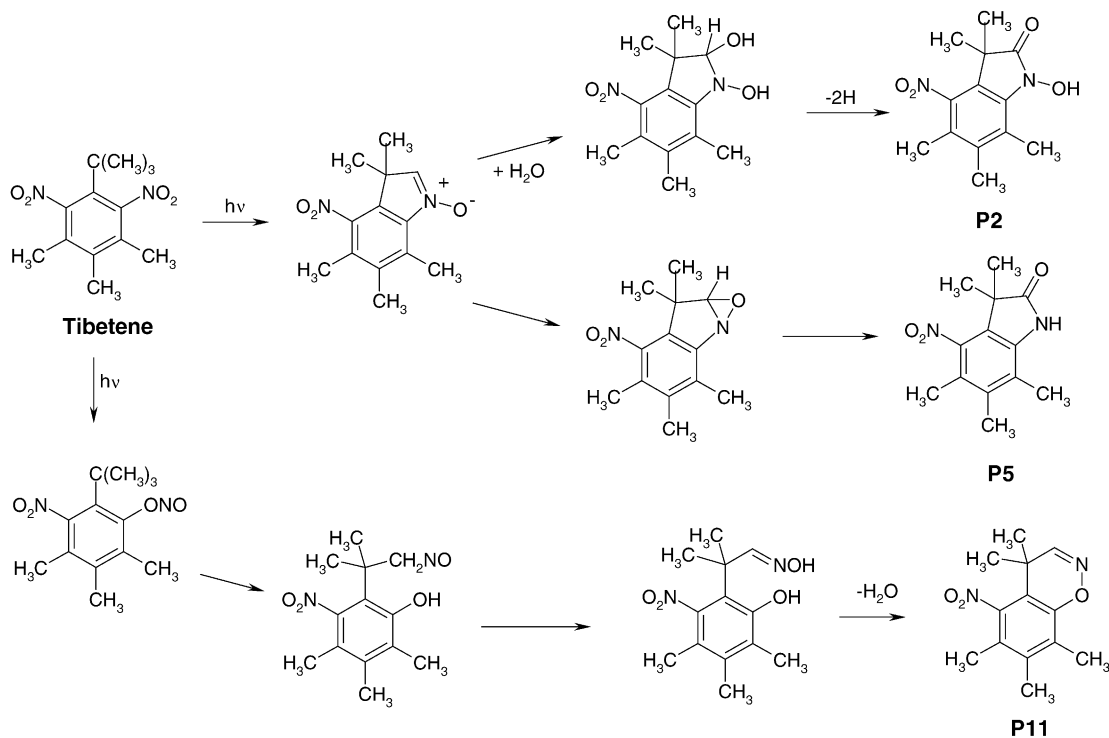
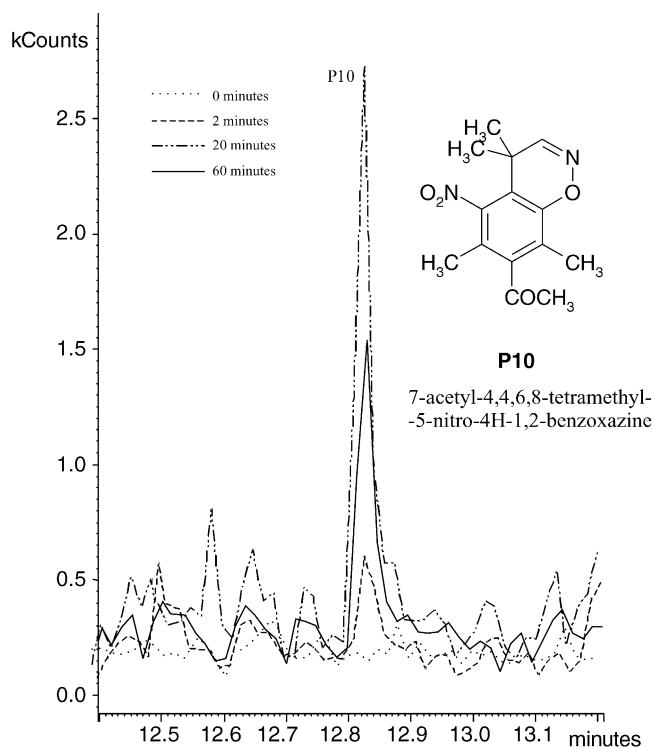Fig. 5. Proposed photodegradation pathways for musk tibetene.

Fig. 6. Chemical structure and ion chromatograms at different irradiation times for the photoproduct detected in the photodegradation of musk ketone (P10).

formation even though the mass spectrometer method was modified on purpose. The main reaction was again photocyclization, leading to photoproducts P8 and P12. P9 is a minor photoproduct obtained by photoreduction of the nitro group.

3.3.3. Tibetene photoproducts

There is not bibliography of photodegradation pathways of musk tibetene either; but, in this case, the idea of an intramolecular reaction similar to that of musk xylene has been suggested by Butte et al. [16]. In fact, in this study three photoproducts (P2, P5 and P11) have been clearly identified, obtained by photocyclization from intramolecular attack of an electronically excited nitro group on the neighbouring *tert*-butyl group (Fig. 5). In the case of P11, there is a previous photorearrangement, before the cyclization of the molecule (Fig. 5).

3.3.4. Ketone photoproducts

Only one photoproduct (P10) has been detected from the photodegradation of musk ketone. This photoproduct was identified by Zhao and Schwack [14] with cyclohexane as the reaction medium as 7-acetyl-4,4,6,8-tetramethyl-5-nitro-4H-1,2-benzoxazine (Fig. 6); and it is originated through nitro-nitrite rearrangement, followed by H-abstraction from the *ortho*-position *tert*-butyl group, then six-membered ring formation and finally water elimination. The correspondent ion chromatograms for three selected irradiation times are also shown in Fig. 6.
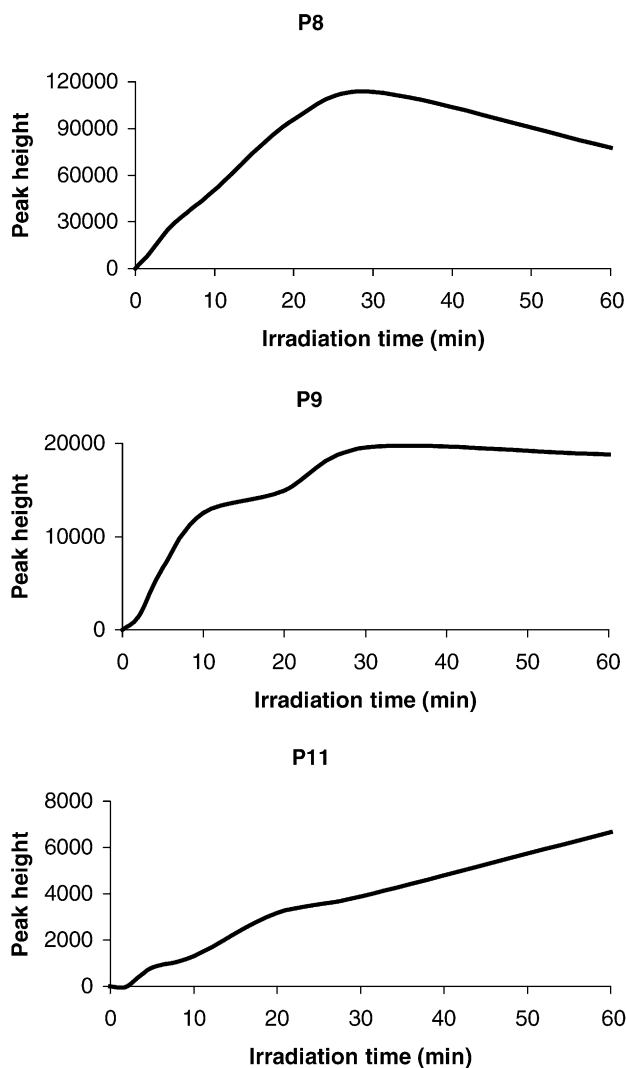

Fig. 7. Photoformation–photodegradation curves for some selected photoproducts.

3.3.5. Other photoproducts

The remaining six photoproducts could not be assigned to any of the proposed photodegradation pathways but all of them have been clearly detected after irradiation of the mixture and individual compounds. In fact, individual studies relate the presence of P1 and P7 with moskene photodegradation and P3, P4, P6 and P13 with tibetene photodegradation (Table 3).

3.4. Photoformation–photodegradation kinetics of the photoproducts

Phototransformation of nitro musks lead to new compounds that also underwent photochemical reactions and the responses (peak height) for some selected compounds at different irradiation times are displayed (Fig. 7). After nitro musks irradiation time of 60 min, all photoproducts can still be detected. Most of them exhibit a maximum peak height at 20–30 min; P8 is a representative compound of such be-

haviour. P9, a photoproduct of moskene, shows a more stable trend. Finally, P11, photoproduct of tibetene, shows a growing trend in the evaluated irradiation time range. The formation during photolysis of products more stable than the nitro musk compounds has already been suggested [16].

References

[1] P.J. Frosch, J.D. Johansen, I.R. White (Eds.), Fragances: Beneficial and Adverse Effects, Springer, Berlin, Heidelberg, 1998.
[2] C.G. Daughton, T.A. Ternes, Environ. Health Persp. 107 (1999) 907.
[3] M. Winkler, J.V. Headley, K.M. Peru, J. Chromatogr. A 903 (2000) 203.
[4] M. Winkler, G. Kopf, C. Hauptvogel, T. Neu, Chemosphere 37 (1998) 1139.
[5] R. Kallenborn, R. Gatermann, S. Planting, G.G. Rimkus, M. Lund, M. Schlabach, I.C. Burkow, J. Chromatogr. A 846 (1999) 295.
[6] J. Hajslová, P. Gregor, V. Chládková, K. Alterová, Organohal. Comp. 39 (1998) 253.
[7] Th. Heberer, S. Gramer, H.J. Stan, Acta Hydrochim. Hydrobiol. 27 (1999) 150.
[8] R. Gatermann, J. Hellou, H. Hühnerfuss, G. Rimkus, V. Zitko, Chemosphere 38 (1999) 3431.
[9] L.I. Osemwengie, S. Steinberg, J. Chromatogr. A 932 (2001) 107.
[10] G.G. Rimkus, W. Butte, H.J. Geyer, Chemosphere 35 (8) (1997) 1497.
[11] Fragances, Draft for Public Hearing, Swedish Society for Nature Conservation, 2000 (http://www.leffingwell.com/rap-bmv-fragrances2000.pdf).
[12] M. Llompart, C. García-Jares, C. Salgado, M. Polo, R. Cela, J. Chromatogr. A 999 (2003) 185.
[13] X. Zhao, W. Schwack, Intern. J. Environ. Anal. Chem. 74 (1998) 179.
[14] X. Zhao, W. Schwack, Toxicol. Environ. Chem. 74 (1999) 217.
[15] X. Zhao, W. Schwack, Chemosphere 39 (1999) 11.
[16] W. Butte, S. Schmidt, A. Schmidt, Chemosphere 38 (1999) 1287.
[17] M. Neamtu, I. Siminiceanu, A. Kettrup, Chemosphere 40 (2000) 1407.
[18] M. Lores, M. Llompart, R. González-García, C. González-Barreiro, R. Cela, Chemosphere 47 (2002) 607.
[19] M. Lores, M. Llompart, R. González-García, C. González-Barreiro, R. Cela, J. Chromatogr. A 963 (2002) 37.
[20] M. Llompart, M. Lores, M. Lourido, L. Sánchez-Prado, R. Cela, J. Chromatogr. A 985 (2003) 175.
[21] L. Sánchez-Prado, M. Lores, M. Llompart, C. García-Jares, M. Lourido, R. Cela, Rapid Commun. Mass Spectr. 18 (2004) 1.
[22] L. Sánchez-Prado, M. Llompart, M. Lores, C. García-Jares, R. Cela, J. Chromatogr. A 1047 (2004) 271.